Chemical Engineering Journal 113 (2005) 55–63

Chemical Engineering Journal

www.elsevier.com/locate/cej

Bactericidal effects of titanium dioxide-based photocatalysts

H.M. Coleman [a], C.P. Marquis [b], J.A. Scott [a], S.-S. Chin [a], R. Amal [a,*]

[a] *Particles and Catalysis Research Group, ARC Centre for Functional Nanomaterials, School of Chemical Engineering and Industrial Chemistry, University of New South Wales, Sydney, NSW 2052, Australia*

[b] *School of Biotechnology and Biomolecular Sciences, University of New South Wales, Sydney, NSW 2052, Australia*

Received 10 March 2005; received in revised form 20 June 2005; accepted 12 July 2005

Abstract

The photocatalytic degradation of *E. coli* in water by various catalysts was investigated in a batch spiral reactor. Commercial Degussa P25 (P25), as well as novel magnetic and hydrothermally prepared photocatalysts (MPC and HPC) were investigated in a slurry system. P25 was found to be the most effective catalyst, followed by the HPC and the MPC. Cell destructions followed first order kinetics. Non-buffered samples displayed a greater bactericidal efficiency which was attributed to a decrease in electrostatic repulsions between TiO_2 and *E. coli* and also elevated stress on *E. coli* at acidic pH. Buffered ($NaHCO_3$) samples showed a decrease in bactericidal efficiency due to HCO_3^- ions competing with oxidising species and blocking (by adsorption) the TiO_2 particles. The optimum catalyst loading for P25 and HPC was 1 and 2 g/L for MPC and was attributed to mass transfer effects (bulk diffusion, available active site and shadowing). An immobilised P25 system was found to be more efficient than the MPC and comparable with the HPC in suspension. The addition of silver to the immobilised system was found to enhance the photocatalytic degradation.

Keywords: Photocatalysis; *E. coli*; Titanium dioxide; Magnetic photocatalyst; Hydrothermal photocatalyst; Immobilised TiO_2; Silver deposited TiO_2

1. Introduction

Chlorination has long been seen as a suitable means for the disinfection of waters for drinking purposes. However, chlorine has a propensity to react with dissolved organic carbon (DOC) initially present in the water to form disinfection by-products (DBPs) [1,2]. Of the wide array of DBPs produced, trihalomethanes (THMs) and haloacetic acids (HAAs) represent the two largest groups [3]. Concern over the formation of these compounds stems from studies indicating they display congenial cardiac defects [3,4] and carcinogenic properties [5,6]. Current Australian Drinking Water Guidelines specify allowable limits of 250 ppb for (total) THMs and 150, 100 and 100 for chloro-, dichloro-, and trichloro-acetic acid, respectively. It is expected that these values will be reduced to conform to those implemented by the US EPA (80 ppb (total) THMs and 60 ppb for the sum of five HAAs [7]) with the potential for further restrictions beyond these to be applied in the future.

As regulations on allowable levels of DBPs in drinking water tighten, alternative technologies capable of meeting these modifications are required. Advanced oxidation processes (AOPs) provide an alternative to chlorination as a disinfection strategy. AOPs such as ozonation and hydrogen peroxide addition are capable of disinfection but possess limitations. Ozonation can lead to DBPs such as bromate [8] and has a short residual residence time [9]. Hydrogen peroxide is a much weaker disinfectant than chlorine or ozone and is subsequently a less favourable option [9]. Photocatalysis is an AOP that has been shown to possess enhanced disinfection capabilities. The non-selective nature of photocatalysis also means it will potentially remove some organics that may be coexisting with the bacteria in solution. The cell killing power of illuminated titania suspensions has been noted since 1988 [10]. Numerous studies have illustrated the effective bactericidal properties of photocatalysis on a diverse range of coliforms [11–13], using various photocatalysts [14–17] and within different reactor systems [18–21].

Heterogeneous photocatalysis utilises a solid semi-conductor (commonly titanium dioxide), either as a suspension of fine particles or immobilised on a support, in conjunction with ultraviolet (UV) radiation to degrade undesirable organic materials. In this work, two methods of application of the photocatalysts

* Corresponding author. Tel.: +61 2 9385 4367; fax: +61 2 9385 5966.
E-mail address: r.amal@unsw.edu.au (R. Amal).

1385-8947/$ – see front matter © 2005 Elsevier B.V. All rights reserved.
doi:10.1016/j.cej.2005.07.015

were used—a slurry type reactor and an immobilised system. The advantages of the slurry type reactor are the large surface area of catalyst and the intimate contact between the target compounds and the suspended particles, reducing mass transfer effects inherent in an immobilised system. The disadvantages are inhibition of light transmittance by the catalyst and the difficulties encountered when attempting to recover the particles from the treated effluent, due to the need for a solid–liquid separation process which is both time and energy consuming. A recently developed magnetic photocatalyst [22,23], comprising insulated magnetic core particles coated with a layer of photoactive titanium dioxide, provides a solution to this problem. The magnetic core allows for increased ease of separation of the particles from the treated effluent whereby the particles can be easily recovered by the application of a magnetic field. The insulative layer (SiO_2) is necessary to prevent interaction between the magnetic cores and the TiO_2, as any interaction leads to the photodissolution of the cores during irradiation [22]. A single-phase nanocrystalline hydrothermally prepared TiO_2 photocatalyst was also produced and assessed for the removal of *E. coli* from water and the effects of solution pH and particle loading of these catalysts investigated. Immobilisation of the catalyst on the reactor walls is a solution to the solid–liquid separation problem. From the point of view of water treatment applications, immobilised TiO_2 has the advantages of easy operation and energy saving. However, the disadvantage of the immobilised system is reduced rate of reaction due to mass transfer effects. One approach that has been applied to increase rates of reaction in TiO_2 photocatalysis is to improve the photoactivity of titania particles by the deposition of metals such as silver, gold, platinum and palladium on the photocatalyst surface [24,25]. The deposition of noble metals on the titania surface has been reported to accelerate both the removal of electrons from the particles and their transfer to molecular oxygen [26]. It has been reported that silver has strong bactericidal effects [27] and as declared by the WHO, silver does not cause adverse health effects setting a secondary minimum concentration level as 90 ppb [28]. In this work silver was photodeposited onto the immobilised TiO_2 and investigated for the photocatalytic degradation of *E. coli* in water to determine if there was any enhancement in rates of bacterial destruction.

2. Experimental section

2.1. Photocatalyst preparation and characterisation

Degussa P25 (P25) (79–21% anatase-rutile [29]) was employed as the commercial source of TiO_2. Hydrothermally prepared single-phased nanocrystalline TiO_2 (100% anatase) (HPC) was prepared for comparison with Degussa P25. Preparation of these particles involves hydrothermally aging an acidified solution containing titanium isopropoxide at 90 °C without further calcination. A detailed preparation procedure for these particles is given by Watson et al. [30].

Preparation of the magnetic photocatalyst (MPC) consists of coating colloidal magnetite particles with an initial layer of SiO_2 and a subsequent layer of TiO_2. The colloidal magnetite particles were prepared according to a method described by Beydoun et al. [31]. The particles were calcined at 450 °C for 3 h to convert the amorphous TiO_2 into photoactive anatase. Calcination also partially oxidises the magnetite to hematite, resulting in a maghemite core. Particle size was determined using a Brookhaven ZetaPlus and particle surface area was determined using nitrogen adsorption on a Micromeritics ASAP 2000.

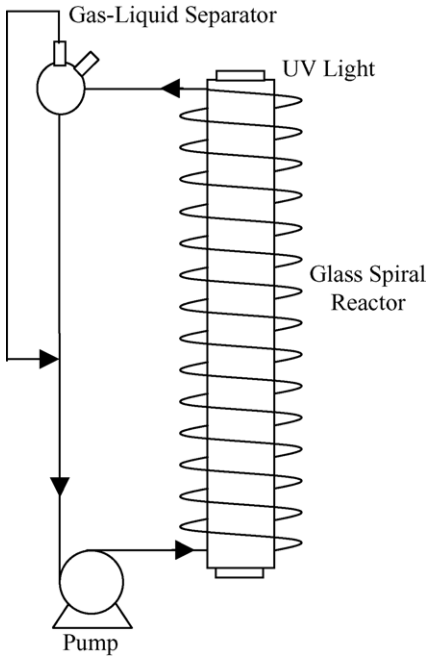

Fig. 1. Schematic of the recirculating glass spiral photocatalytic reactor.

2.2. Reactor set ups

All reactors were illuminated by a 20 W black-light-blue lamp (NEC Brand), located within the centre of each reactor coil. The lamps emit radiation over a wavelength range of 320–420 nm with a maximum emission at 360 nm.

2.2.1. Slurry systems—P25, HPC and MPC

For P25, HPC and the MPC slurry systems, bactericidal studies were undertaken in recirculating glass spiral reactors as illustrated in Fig. 1. The reactors were constructed using borosilicate glass tubing of 6 mm outer diameter and 1 mm wall thickness. The total volume available for illumination was 70 mL per reactor. A gas–liquid separator was located within each circuit where gas was drawn off the line and re-injected at a later stage (see Fig. 1). This arrangement facilitated a plug-flow reactor system which aided solution aeration and particle suspension. The slurry was circulated through each reactor by a triple-head peristaltic pump (Masterflex Quick-load, Cole-Palmer Instrument Co.) using Masterflex tubing at a flow rate of 220 mL/min.

2.2.2. Immobilised systems—P25 and Ag/P25

The photocatalytic experiments were carried out in a glass borosilicate spiral reactor (volume = 85 mL) similar to the slurry reactors (Fig. 1) except the TiO_2 catalyst was immobilised onto the inside wall of the reactor. The glass coil reactor

was connected to a peristaltic pump (Masterflex® Quick-Load, Cole-Palmer Instrument Co.) by Masterflex flexible tubing to enable solution circulation through the reactor at a flow rate of 220 mL/min.

The TiO_2 was immobilised by first filling the reactor with 20% hydrofluoric acid for 1 h to etch the inside surface of the reactor. A 1% wt./vol. solution of TiO_2 (sonicated in an ultrasonic bath for 20 min) was then pumped through the reactor and allowed to stand for approximately 1 h, drained and dried in an oven at 60 °C. This process was repeated 3–4 times. A thin film of TiO_2 was formed on the inside wall of the reactor. The immobilisation of silver metal onto the TiO_2 particles was carried out by photodeposition. Based on previous findings [32,33] a 2 atom percent (at.%) silver loading was used. Silver nitrate was used as the source of silver. A known calculated amount of $AgNO_3$ was added to 85 mL of 100 μg/L formic acid to give a final concentration of 2 at.% Ag^+ in the glass coil reactor containing the immobilised TiO_2 and circulated in the dark for 15 min to allow the system to equilibrate. The UV lamp was then turned on and the solution was circulated for 2 h to allow photooxidation of the formic acid and photoreduction of the metal ions to occur.

2.3. Microbiology

Escherichia coli (*E. coli*) (strain HB101) was used as the test strain for all bacterial inactivation studies. Single colonies were isolated from Luria Bertani agar plate cultures (10 g/L Tryptone, 5 g/L Yeast Extract, 5 g/L NaCl, 15 g/L agar) and used to inoculate 50 mL of Luria Bertani liquid media (10 g/L Tryptone, 5 g/L Yeast Extract, 5 g/L NaCl) in a 500 mL baffled Erlenmeyer flask. The flask was incubated overnight at 30 °C on an orbital shaker at 200 rpm. The next day, the culture was refreshed by pipetting 5–10 mL into a second 500 mL Erlenmeyer flask containing 50 mL of nutrient broth and leaving on the shaker for 2–3 h to ensure maximum cell viability prior to commencing each experiment.

2.4. Bactericidal activity

Autoclaved "MilliQ" (Millipore) water (18 MΩ/cm^2) supplemented with filter sterilised sodium hydrogen carbonate (to 0.06 g/L) buffer was used for all inactivation experiments. For slurry reactions, sufficient catalyst was added to the buffered solution to give the required loading. The pH was adjusted to 7.0 ± 0.3 and the *E. coli* added to the suspension to give the desired initial cell density. 45 mL of the prepared solution (for slurry reactions) or 110 mL of buffer and *E. coli* (for the immobilised system) was introduced to the reactor and circulated for 8 min prior to irradiation. Samples were taken at defined time intervals for analysis.

2.5. Analysis

Bacterial cell density in liquid media was estimated using absorbance at 600 nm on a UV–vis spectrophotometer (Pharmacia). Based on this cell density estimation, the inoculum was diluted and used to inoculate the reactor prior to the experiment, aiming to commence each experiment at a cell density of 2500 cfu/mL.

Cell density in the reactors was calculated using the viable plate count method. Three 100 μL samples were micropipetted from the reactor and plated onto three respective agar plates and spread over the agar surface using a plate spreader. Plates were then incubated overnight at 37 °C and colonies were observed and counted the next morning. An average count was calculated from the three plate counts and results were plotted as percentage survival over time. The first order rate constants for each experiment were calculated from plots of $\ln C/C_0$ (where C is the concentration and C_0 is the initial concentration) over time.

2.6. Parameters investigated

The effect of buffer on cell death was considered for the catalysts in suspension. Solution preparation was identical to that described earlier (Section 2.4) but without the presence of the sodium hydrogen carbonate buffer. The catalyst loading typically used for all three photocatalysts in suspension was 1 g/L. The effect of catalyst loading on bacteria removal was determined by varying the catalyst concentration over the range 0–2 g/L for P25, HPC and MPC. The effect of immobilising Degussa P25 on the reactor walls was investigated for the degradation of *E. coli* in water and compared with results obtained for reactions in suspension. The effect of photodepositing 2 at.% Ag on the immobilised TiO_2 (P25) was investigated for the removal of *E. coli* from water. Control experiments were carried out with UV light alone and photocatalyst in the dark.

3. Results and discussion

3.1. Effect of photocatalyst – reactions in suspension – P25, HPC and MPC

The results obtained for particle size and surface area of all three catalysts are shown in Table 1.

Table 1 shows that the photocatalysts consisted primarily of anatase. Degussa P25 also contains approximately 21% rutile. Also noticeable from Table 1 is the much larger particle size of MPC relative to the other photocatalysts. The TEM images of the three photocatalysts are shown in Fig. 2 [34]. The larger particle size of MPC results from aggregation of the magnetic particles during the silica coating process and agglomeration during the calcination process (as shown in Fig. 2(a)). Of the three samples, HPC has a substantially larger surface area than

Table 1
Particle characteristics for the commercial (P25) and prepared TiO_2 (HPC and MPC) photocatalysts

Sample	TiO_2 crystal phase	Diameter[a] (nm)	Surface area (m^2/g)
P25	79% anatase, 21% rutile [29]	200	55
HPC	Anatase	180	302
MPC	Anatase (coating)	1060	90

[a] Corresponds to particle diameter in suspension.

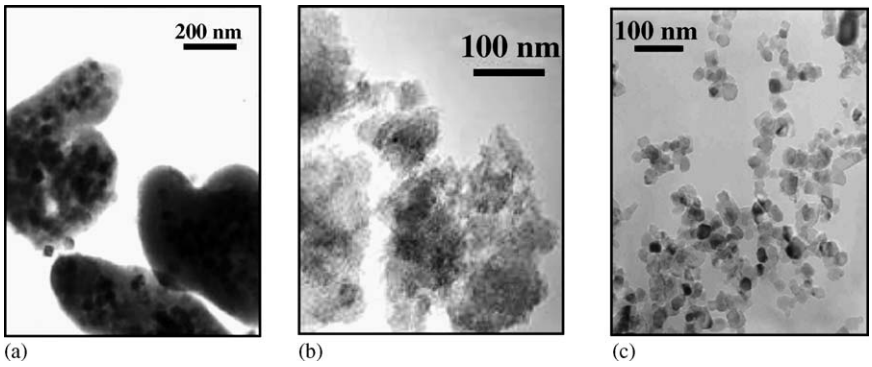

Fig. 2. TEM images of (a) MPC, (b) HPC and (c) Degussa P25 [34]. The ability of the three photocatalysts P25, HPC and MPC to inactivate *E. coli* in water was investigated with the results shown in Fig. 3.

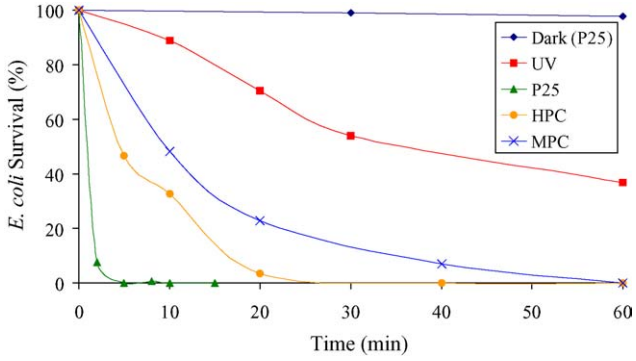

Fig. 3. Bactericidal effect of different TiO_2 samples for the removal of *E. coli*. P25: Degussa P25, HPC: hydrothermal photocatalyst, MPC: magnetic photocatalyst, dark (P25): absence of UV irradiation, UV: absence of TiO_2. Catalyst loading 1 g/L, pH 7–7.8 (buffered using $NaHCO_3$), initial colony count ≈2500 cfu/mL.

the other two samples. This high surface area is due to the large internal surface area of the particles, created by the aggregation and bonding of many small anatase crystals during preparation (see Fig. 2(b)).

The ability of the three photocatalysts P25, HPC and MPC to inactivate *E. coli* in water was investigated with the results shown in Fig. 3. Included are the control experiments—UV light alone (i.e., no photocatalyst) and TiO_2 (P25) alone (i.e., under dark conditions). The initial inactivation follows a first order dependence agreeing with previous studies on photocatalysis of *E. coli* in water using Degussa P25 [11,12,14,35–39]. The first order rate constants for each reaction were calculated and are shown in Table 2. Standard errors were calculated from the log linear regression function.

Fig. 3 indicates that there is no effect of TiO_2 (P25) alone (dark conditions) on *E. coli* degradation, indicating no adsorption of *E. coli* on the TiO_2 or reactor walls. Similar results were obtained for HPC and MPC under dark conditions. UV light alone demonstrated bactericidal properties as expected [35] but was much less efficient than photocatalysis, with 37% of the initial *E. coli* still viable after 60 min exposure. All three photocatalysts displayed bactericidal properties upon irradiation. Of the three samples, P25 was found to be the most efficient (100% *E. coli* removal within 10 min irradiation). HPC required around 40 min for complete removal, while MPC took 60 min to kill all *E. coli*. This can be seen clearly from the calculated first order rate constants in Table 2. The most effective photocatalyst was Degussa P25 which was almost 8 times faster than HPC and 20 times faster than MPC in degrading *E. coli*. HPC is 2.5 times faster than MPC. The observed results can be related to the particle size and density of the catalysts. MPC has a larger particle size and is also denser due to the magnetic core, hence has a lower available particle population (per mL) for reaction. P25 and HPC have similar particle sizes but P25 is more active. It has previously been shown that P25 is more active than HPC and MPC for the photocatalysis of sucrose [30]. Degussa P25 is well known for its high activity which may be due to its better crystallinity as dispersed nano-TiO_2 particles may interact better with *E. coli*. Cell wall damage followed by cytoplasmic membrane damage leading to a direct intracellular attack has been proposed as the sequence of events when microorganisms undergo TiO_2 photocatalytic attack. It has been found that smaller TiO_2 particles cause quicker intracellular damage [40].

Table 2
Rate constants for photocatalysis of *E. coli* in water

Photocatalyst	Rate constant, k (min^{-1})
Degussa P25	1.32 ± 0.28
Hydrothermal Photocatalyst (HPC)	0.166 ± 0.011
Magnetic photocatalyst (MPC)	0.066 ± 0.003

3.2. Effect of buffer

The effect of buffering the pH of the solution (pH 7–7.8) on the bactericidal efficiency was investigated. The pH values of the buffered and non-buffered solutions prior to and following 1 h irradiation are given in Table 3.

Table 3 indicates that if the solution is not buffered then upon irradiation the pH drops and the solution becomes acidic. The pH drop maybe due to two phenomena. TiO_2 in suspension has a pH of about 5 [41]. Even in the absence of bacteria, illuminated TiO_2 leads to a decrease of pH 7.0 to 5.5 due to the following reaction [42]:

$$H_2O + h^+ (TiO_2) \rightarrow {}^{\bullet}OH + H^+ \quad (1)$$

The pH drop could also be due to aliphatic acids being produced when endo- and exo-bacterial organic compounds are photo-

Table 3
Changes in solution pH following irradiation of (sodium hydrogen carbonate) buffered and non-buffered solutions of Degussa P25, HPC and MPC[a]

Photocatalyst	pH with buffer		pH without buffer	
	Before irradiation	Following irradiation	Before irradiation	Following irradiation
P25	7.1	7.0	7.4	5.1
HPC	7.4	7.5	7.2	4.1
MPC	7.3	7.3	7.2	5.6

[a] Catalyst loading 1 g/L, irradiation time 60 min, initial colony count ≈2500 cfu/mL. Initial pH of non-buffered solution adjusted using sodium hydroxide.

catalytically oxidised by hydroxyl radicals ($^{\bullet}$OH) and radical oxygenated species (ROS) during the photocatalytic treatment [42].

endo- and exo-bacterial organic compounds

$$+\,\mathrm{OH},\ \mathrm{ROS} \rightarrow \text{aliphatic acids} \quad (2)$$

The impact of buffering the solution to a pH of 7–7.8 on the bactericidal efficiency of P25, HPC and MPC is shown in Fig. 4.

It is observed from Fig. 4 that unbuffered solutions display a greater bactericidal efficiency for each of the photocatalysts. The greater rate of *E. coli* removal is a result of the accompanying drop in solution pH during irradiation. *E. coli* is most viable within a pH range of 6–8 [42] and the additional stress encountered under acidic conditions leads to an acceleration of the rate of *E. coli* inactivation. Research [38] with urban waste waters showed that acidic conditions (pH 5) enhanced photocatalytic deactivation of *E. coli.* At acidic pH the electrostatic repulsion between TiO_2 and *E. coli* is not as great i.e., the surface charge of TiO_2 is more neutral which allows increased interaction between TiO_2 and the bacteria. However, there is not as a significant effect with P25 compared to the other catalysts. This is due to the high bactericidal activity of P25. The rate of reaction for P25 is already high under buffered conditions so there is not as a significant difference in unbuffered conditions.

The decrease in deactivation rates of *E. coli* in buffered solutions may also be due to the presence of HCO_3^- ions (from the $NaHCO_3$ buffer) which retard the *E. coli* deactivation rates by competing with the oxidising radicals or by blocking (adsorbed on TiO_2) the active sites of the TiO_2 catalyst [42]. HCO_3^- reacts with the hydroxyl radicals producing the less reactive anion radical $CO_3^{\bullet -}$.

$$HCO_3^- + OH \rightarrow H_2O + CO_3^{\bullet -} \quad (3)$$

This radical shows a wide range of reactivity with organic molecules but it is mainly a selective electrophilic reagent, and its reactions are slower than those of $^{\bullet}$OH. HCO_3^- also provides some photoadsorption that protects bacteria towards light [42]. This screening effect added to the one created by TiO_2 particles, limits the light penetrated into the bacterial suspensions. HCO_3^- ions could also act as scavengers of holes (h^+) formed on the TiO_2 surface reducing the inactivation rate [43].

$$h^+ + HCO_3^- \rightarrow HCO_3^{\bullet -} \quad (4)$$

3.3. Catalyst loading

The effect of catalyst loading on the photobactericidal performance of P25, HPC and MPC are shown in Figs. 5–7, respectively. The values obtained for rate constants are shown in Table 4.

Fig. 5 indicates that the optimum loading for P25 is 1 g/L. Degradation rates are 1 g/L > 2 g/L > 0.5 g/L (see Table 4) with 1 and 2 g/L being very similar. A loading of 0.5 g/L leads to a noticeable reduction in efficiency with complete colony removal taking 30 min. A loading of 2 g/L presented only a minor decrease in the photobactericidal efficiency of P25 and is very similar to the degradation rate of 1 g/L. Fig. 6 indicates that a reduction in HPC loading to 0.5 g/L resulted in *E. coli* bacteria still being present after 60 min irradiation. Degradation rates were in the order 1 g/L > 2 g/L > 0.5 g/L (Table 4) showing a similar trend to Degussa P25. Increasing the loading to 2 g/L also

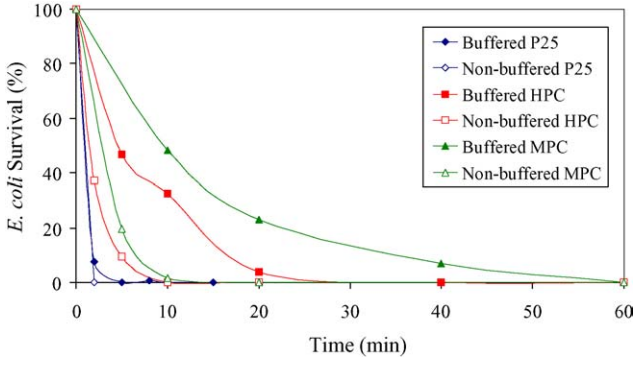

Fig. 4. The effect of buffering (sodium hydrogen carbonate) the initial solution on the bactericidal efficiency of Degussa P25, HPC and MPC. Catalyst loading 1 g/L, initial solution pH buffered to 7–7.8, initial colony count ≈2500 cfu/mL.

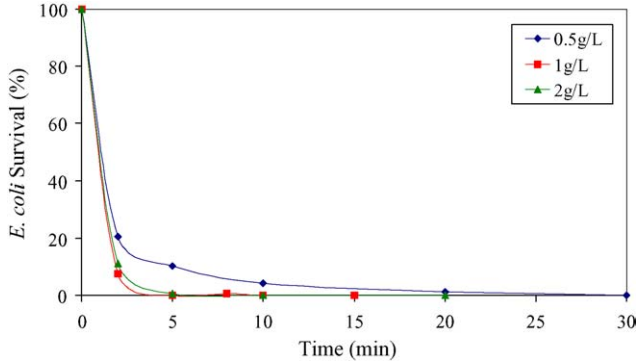

Fig. 5. Effect of catalyst loading on bactericidal efficiency of Degussa P25. Catalyst loadings considered were 0.5, 1 and 2 g/L. pH 7–7.8, initial colony count ≈2500 cfu/mL.

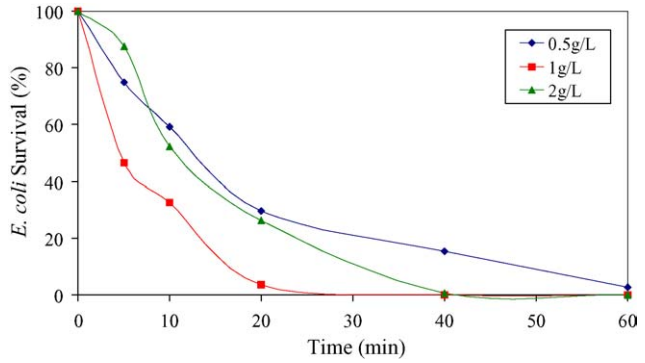

Fig. 6. Effect of catalyst loading on the photobactericidal efficiency of HPC. Catalyst loadings considered were 0.5, 1 and 2 g/L. pH 7–7.8, initial colony count ≈2500 cfu/mL.

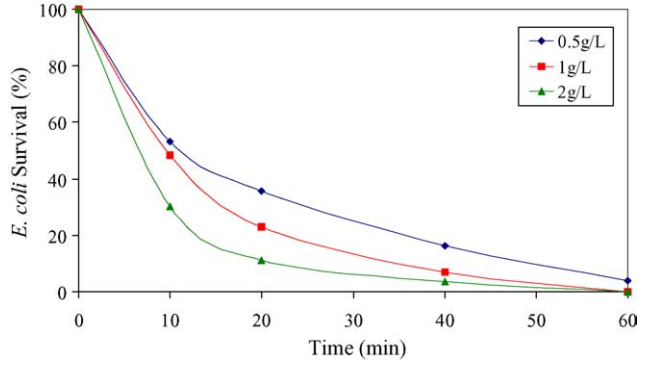

Fig. 7. Effect of catalyst loading on the photobactericidal efficiency of MPC. Catalyst loadings considered were 0.5, 1 and 2 g/L, pH 7–7.8, initial colony count ≈2500 cfu/mL.

lead to a poorer removal efficiency compared to the 1 g/L loading. These particles are of a similar size to P25 so dispersion characteristics are expected to be similar. Increasing Degussa from 1 to 2 g/L only decreases the rate slightly, but increasing HPC from 1 to 2 g/L affects the deactivation rate significantly. This decrease in rate with loading may be attributed to the rough surface of HPC [34] which would cause increased light scatter at higher loadings. Fig. 7 indicates that as the MPC loading increases from 0.5 to 2 g/L so too does the bactericidal efficiency. Degradation rates were of the order 2 g/L > 1 g/L > 0.5 g/L (see Table 4). This is a different trend to that observed for P25 and HPC, indicating that the optimum loading also depends on the photocatalyst properties.

Table 4
Rate constants at different catalyst loadings for photocatalytic degradation of *E. coli*

Photocatalyst	Rate constant, k (min^{-1})		
	0.5 g/L	1 g/L	2 g/L
Degussa P25	0.194 ± 0.046	1.32 ± 0.28	1.03 ± 0.10
Hydrothermal photocatalyst (HPC)	0.058 ± 0.005	0.166 ± 0.011	0.068 ± 0.002
Magnetic photocatalyst (MPC)	0.051 ± 0.004	0.066 ± 0.003	0.081 ± 0.011

From Figs. 5–7 and Table 4, it is apparent that for P25 and HPC, a photocatalyst loading of 1 g/L provides the greatest bactericidal efficiency. The decrease in efficiency at loadings lower than 1 g/L is due to mass transfer effects (i.e., there are a lower number of particles available to interact with the *E. coli*). At loadings higher than 1 g/L the higher number of particles amplify the light scattering and shadowing effects, reducing the extent to which the UV light can reach all the particles in suspension. The loading effects for MPC are different, due essentially to the larger size (see Table 1) and increased weight of the particles (due to the magnetic core) compared to the other TiO_2 samples. These factors give a lower particle number density for MPC (i.e., less particles are available per mL of solution). At the loadings investigated for MPC, mass transfer effects dominate as the lower particle number density controls the reaction rate. It is expected that at higher MPC loadings, light scattering and shadowing effects will begin to exert an influence.

Bekbolet et al. [36,37] investigated the effect of TiO_2 (P25) loading on the inactivation of *E. coli.* in the range 0–1.5 g/L and found 1 g/L to be the effective optimum concentration. The effect of loadings in the range 0.25–2.5 g/L at different initial counts (10^2 to 10^4 cells/mL) revealed the same optimum effective concentration. Maness et al. [44] also found that the most effective TiO_2 (P25) concentration for killing *E. coli* cells at concentrations ranging from 10^3 to 10^8 cfu/mL to be 1 g/L. Rincon and Pulgarin [45] investigated the influence of TiO_2 concentration on *E. coli* inactivation in the range of 0.25–1.5 g/L and also found that initial rates increase with the amount of catalyst to a plateau at 1 g/L and attributed it to the complete absorption of the incident light by TiO_2. Rates at 1.5 g/L were very similar to 1 g/L. Thus, at TiO_2 concentrations higher than 1 g/L, the weak light penetration into the bulk of the solution makes the photoactivity of the catalyst less effective and the action of light on bacteria (direct photolysis) is also diminished. This is similar to our findings where loadings of 2 g/L have similar rates to 1 g/L. The optimal concentration for wastewater was 0.5 g/L compared to 1 g/L for MilliQ water suggesting that the optimal TiO_2 concentration depends also on the chemical matrix of the water. A more detailed study by Cho et al. [35] investigated the optimum conditions for *E. coli* disinfection from 0.1 to 5 g/L of TiO_2. Above 1 g/L TiO_2 concentration, the disinfection reaction was less effective because TiO_2 particles may result in screening of the light. At lower TiO_2 loadings, much of the light was transmitted through the slurry solution in the reactor, while at higher catalyst loadings all the incident photons were absorbed by the slurry. There was not much difference in the survival ratio for TiO_2 loadings of range from 1 to 5 g/L. The efficiency was probably limited over 1 g/L of TiO_2 because UV light can be blocked by the TiO_2 catalyst itself. Thus, it seems reasonable to conclude that 1 g/L loading is sufficient to harvest all of the incident light and that there is no advantage in going beyond this catalyst loading.

3.4. Effect of immobilising titanium dioxide (P25)

Degussa P25 was shown to be the most efficient catalyst for the removal of *E. coli* in water and was much more efficient

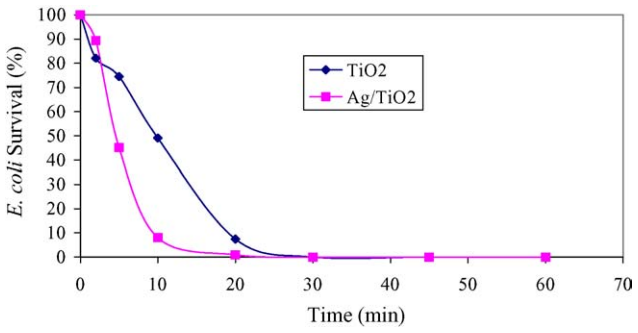

Fig. 8. Bactericidal effects of immobilised TiO_2 (P25) and Ag/TiO_2. Silver loading 2 at.%, initial solution pH buffered to 7–7.8, initial colony count ≈2500 cfu/mL.

than the magnetic photocatalyst. To overcome the problems of filtration and removal of the catalyst after reaction, Degussa P25 was immobilised onto the reactor walls and this system assessed for the removal of *E. coli* in water. A typical decay curve for the immobilised system along with a typical decay curve for the silver/TiO_2 system is shown in Fig. 8. The reactions were seen to exhibit first order behaviour. The first order rate constants were calculated and are shown in Table 5.

Comparing the results for the immobilised catalyst (Table 5) with optimum results (i.e. 1 g/L loadings for P25 and HPC and 2 g/L for MPC) for the catalysts in suspension (Table 2), it can be seen that the immobilised P25 is not as efficient as the P25 in suspension. This is due to mass transfer effects and the larger surface area available for reaction for particles in suspension. However, the immobilised P25 is comparable to rates for the HPC and is much more efficient than the MPC (almost twice the rate for MPC). These results indicate that it is therefore much more efficient to use an immobilised system for practical and commercial applications as lengthy and expensive filtration and separation steps are eliminated. Control experiments of immobilised TiO_2 in the dark showed no change in *E. coli* indicating that there is no adsorption of *E. coli* on the TiO_2 or the reactor walls.

3.5. Effect of the addition of Ag

It can be seen from Fig. 8 and the rate constants in Table 5 that the addition of silver enhances the degradation of *E. coli* compared to TiO_2 alone. The rate is 1.6 times greater on the addition of silver indicating that the silver/TiO_2 is a more effective antibacterial material than uncoated TiO_2 under UV irradiation. There is no bactericidal effect observed with Ag/TiO_2 in the dark. These results are in agreement with previous work by Sokmen et al. [17] and Zhang et al. [46] who investigated the effect of silver/TiO_2 on the photokilling of *E. coli* and *M. lylae* in water, respectively. The enhancement on the addition of silver may be attributed to silver's ability to act as an electron trap, reducing recombination of electrons and holes and thus favouring oxidative attack on the *E. coli.* This enhancing effect of silver/TiO_2 has been observed for the photocatalytic degradation of many organic substrates in water [17,32,47–62]. The increase in reaction rate may also be due to the bactericidal properties of silver which, combined with photocatalytic attack enhance the reaction. The development of TiO_2 immobilised photoreactor systems have gained great interest which leads to physical and chemical modifications of TiO_2 to improve the catalyst performance. It is well known that silver ions have bacteriostatic/bactericidal effects [27]. Therefore, loading TiO_2 with silver was thought to increase the effectiveness of this catalyst system. Sokmen et al. [17] reported that silver loading (2 at.%) dramatically reduced the illumination time for complete degradation of *E. coli* in water. They suggested the presence of silver ions enhanced the reaction rate by trapping the conducting band electrons besides reducing the band gap energy of titanium dioxide. Zhang et al. [46] observed enhanced photocatalytic and bactericidal properties of TiO_2 on the addition of silver. Rates were 1.3 times faster for the photokilling of the bacteria *M. lylae.* They also observed no bactericidal effect in the dark with either Ag/TiO_2 or TiO_2 alone. They attributed the enhancement to better charge separation arising from loading of silver nanoclusters and also to the bactericidal properties of silver. It has also been suggested that Ag^+ interacts with the sulphydryl groups of respiratory enzymes in the plasma membranes of susceptible bacteria [62]. This respiratory enzyme-binding leads to changes in membrane permeability, which has been known to cause changes in the cell body, including detachment of the plasma membrane from the cell wall. When a solid support containing Ag metal is placed in a suspension, the Ag^+ released from the surface can kill bacteria [63]. Keleher et al. [63] found that Ag/TiO_2 particles were shown to have a greater inhibitory effect on *E. coli* than Ag metal. They attributed this to the efficiency of the Ag metal dissolution to Ag^+ and the subsequent diffusion of the Ag^+ to the bacteria membrane [17].

From currently available evidence and their own work, Huang et al. [40] proposed a detailed mechanism for the bactericidal effect of the TiO_2 photocatalytic reaction. The initial oxidative damage takes place on the cell wall, where the TiO_2 photocatalytic surface makes first contact with intact cells. Cells with a damaged cell wall are still viable. After eliminating the protection of the cell wall, the oxidative damage takes place on the underlying cytoplasmic membrane. Photocatalytic action progressively increases the cell permeability and subsequently allows the free efflux of intracellular contents that eventually leads to cell death. Free TiO_2 particles may also gain access into membrane-damaged cells, and the subsequent direct attack on the intracellular components can accelerate cell death. In a mechanistic study on the antibacterial effect of silver ions on *E. coli* and *Staphylococcus aureus,* significant morphological changes were reported in *E. coli* cells after the addition of Ag^+ [27]. The cytoplasm membrane shrank or became detached from the cell wall and silver ions were detected inside the cells.

Table 5
Rate constants for photocatalysis of *E. coli* over immobilised TiO_2 (Degussa P25) and Ag/TiO_2 (Degussa P25)

Photocatalyst	Rate constant, k (min^{-1})	Standard error
TiO_2	0.125 (four runs)	0.018
Ag/TiO_2	0.200 (five runs)	0.016

There is yet to be a detailed study on the effects of Ag/TiO_2 on *E. coli* bacteria and the mechanism involved. However, from the evidence presented, it seems the TiO_2-mediated photocatalytic attack combined with silver's 'electron trapping' and bactericidal properties give a more efficient treatment method than Ag or TiO_2 photocatalysis alone. In a practical situation, it is therefore viable to add silver to an immobilised TiO_2 system since the bactericidal efficiencies have been significantly enhanced.

4. Conclusions

Photocatalysis is effective for removing *E. coli* in water using titanium dioxide Degussa P25, a hydrothermal photocatalyst (HPC) and a magnetic photocatalyst (MPC). P25 was found to be the most effective catalyst, followed by the HPC and finally the MPC. Non-buffered water samples displayed a greater bactericidal efficiency. This was attributed to a decrease in electrostatic repulsions between TiO_2 and *E. coli* and elevated stress on *E. coli* at acidic pH. Buffered samples showed a decrease in bactericidal efficiency. This was attributed to the presence of HCO_3^- ions which compete with oxidising species and also block the TiO_2 particles. The optimum catalyst loading for P25 and HPC were determined as 1 and as 2 g/L for MPC. This was attributed to factors such as bulk diffusion, available active sites and shadowing effects. An immobilised TiO_2 P25 system was found to be effective in removing *E. coli* from water. It was much more efficient than the MPC catalyst, was comparable with HPC but is not as effective as P25 in suspension. However, from a practical point of view, it is much more efficient as costs can be reduced from separation and filtration of the catalyst. The addition of silver to the immobilised system was found to enhance the photocatalytic degradation. This may be attributed to the ability of silver to act as an electron trap and prevent recombination of electrons and holes in the photocatalytic process and also its bactericidal properties. It can therefore be concluded that, for practical applications an immobilised Ag/TiO_2 catalyst is the most effective for the photocatalytic removal of *E. coli* from water.

Acknowledgement

Dr. Jeff Welch from the School of Biotechnology and Biomolecular Sciences, University of New South Wales for supplying the *E. coli* strain.

References

[1] E.R. Blatchley III, D. Margetas, R. Duggirala, Water Res. 37 (2003) 4385–4394.
[2] K.L. Simpson, K.P. Hayes, Water Res. 32 (5) (1998) 1522–1528.
[3] M.I. Cedregren, A.J. Selbing, O. Löfman, B.A.J. Källen, Environ. Res. Sect. A 89 (2002) 124–130.
[4] C.G. Graves, G.M. Matanoski, R.G. Tardiff, Regul. Toxicol. Pharmacol. 34 (2001) 103–124.
[5] J. Kim, Y. Chung, D. Shin, M. Kim, Y. Lee, Y. Lim, D. Lee, Desalination 151 (2002) 1–9.
[6] J. Milot, M.J. Rodriguez, J.B. Serodes, J. Environ. Manage. 60 (2000) 155–171.
[7] P.C. Singer, Water Sci. Technol. 40 (9) (1999) 25–30.
[8] X. Zhang, S. Echigo, H. Lei, M.E. Smith, R.A. Minear, J.W. Talley, Water Res. 39 (2005) 423–425.
[9] B.R. Kim, J.E. Anderson, S.A. Mueller, W.A. Gaines, A.M. Kendall, Water Res. 36 (2002) 4433–4444.
[10] D.F. Ollis, Photocatalytic purification and remediation of contaminated air and water, C.R. Acad. Sci. Paris, Ser. IIc: Chim./Chem. 3 (2000) 405–411.
[11] J.A. Ibanez, M.I. Litter, R.A. Pizarro, J. Photochem. Photobiol. A: Chem. 157 (2003) 81–85.
[12] K.P. Kuhn, I.F. Chaberny, K. Massholder, M. Stickler, V.W. Benz, H.-G. Sonntag, L. Erdinger, Chemosphere 53 (2003) 71–77.
[13] B. Kim, D. Kim, D. Cho, S. Cho, Chemosphere 52 (2003) 277–281.
[14] H.-L. Liu, T.C.-K. Yang, Process Biochem. 39 (2003) 475–481.
[15] K. Sunada, T. Watanabe, K. Hashimoto, Environ. Sci. Technol. 37 (2003) 4785–4789.
[16] T. Tatsuma, S. Takeda, S. Saitoh, Y. Ohko, A. Fujushima, Electrochem. Commun. 5 (2003) 793–796.
[17] M. Sokmen, F. Candan, Z. Sumer, J. Photochem. Photobiol. A: Chem. 143 (2001) 241–244.
[18] F. Shiraishi, K. Toyoda, S. Fukinbara, E. Obuchi, K. Nakano, Chem. Eng. Sci. 54 (1999) 1547–1552.
[19] Y.-S. Choi, B.-W. Kim, J. Chem. Technol. Biotechnol. 75 (2000) 1145–1150.
[20] D.D. Sun, J.H. Tay, K.M. Tan, Water Res. 37 (2003) 3452–3462.
[21] Y. Horie, M. Taya, S. Tone, J. Chem. Eng. Jpn. 31 (4) (1998) 577–584.
[22] D. Beydoun, R. Amal, G. Low, S. McEvoy, J. Mol. Catal. A: Chem. 180 (2002) 193–200.
[23] D. Beydoun, R. Amal, J. Scott, G. Low, S. McEvoy, Chem. Eng. Technol. 24 (7) (2001) 745–748.
[24] K.A. Magrini, A. Watt, B. Rinehart, in: W.B. Stine, T. Tanaka, D.E. Claridge (Eds.), Solar Engineering, vol. 1, The American Society of Mechanical Engineers, 1995, pp. 415–420.
[25] D. Hufschmidt, D. Bahnemann, J.J. Testa, C.A. Emilio, M.I. Litter, J. Photochem. Photobiol. A 148 (1–3) (2002) 223–231.
[26] H. Gerischer, A. Heller, J. Electrochem. Soc. 139 (1992) 113.
[27] Q.L. Feng, J. Wu, G.Q. Chen, F.Z. Cui, T.N. Kim, J.O. Kim, J. Biomed. Mater. Res. 52 (2000) 662–668.
[28] R. Pedahzur, O. Lev, B. Fattal, H.I. Shuval, Water Sci. Technol. 31 (1995) 123–129.
[29] K. Chiang, R. Amal, T. Tran, Adv. Environ. Res. 6 (2002) 471–485.
[30] S. Watson, D. Beydoun, R. Amal, J. Photochem. Photobiol. A: Chem. 148 (1–3) (2002) 303–313.
[31] D. Beydoun, R. Amal, G.K.-C. Low, S. McEvoy, J. Phys. Chem. B 104 (18) (2000) 4387–4396.
[32] V. Vamathevan, R. Amal, D. Beydoun, G. Low, S. McEvoy, J. Photochem. Photobiol. A: Chem. 148 (2002) 233–245.
[33] V. Vamathevan, R. Amal, D. Beydoun, G. Low, S. McEvoy, Chem. Eng. J. 98 (2004) 127–139.
[34] S. Watson, Ph.D. Thesis, ARC Centre for Functional Nanomaterials, School of Chemical Engineering and Industrial Chemistry, University of New South Wales, Sydney, Australia, 2005.
[35] I.-H. Cho, I.-Y. Moon, M.-H. Chung, H.-K. Lee, K.-D. Zoh, Water Sci. Technol.: Water Supply 2 (1) (2002) 181–190.
[36] M. Bekbolet, C.V. Araz, Chemosphere 32 (5) (1996) 959–965.
[37] M. Bekbolet, Water Sci. Technol. 35 (11–12) (1997) 95–100.
[38] J.A. Herrera Melian, J.M. Dona Rodriguez, A. Viera Suarez, A.E. Tello Rendon, C. Valdes do Campo, J. Arana, J. Perez Pena, J. Chemosphere 41 (2000) 323–327.
[39] P.S.M. Dunlop, J.A. Byrne, N. Manga, B.R. Eggins, J. Photochem. Photobiol. A: Chem. 148 (2002) 355–363.
[40] Z. Huang, P.-C. Maness, D.M. Blake, E.J. Wolfrum, S.L. Smolinski, W.A. Jacoby, J. Photochem. Photobiol. A: Chem. 130 (2000) 163–170.
[41] M.R. Hoffman, S.T. Martin, W. Choi, D.W. Bahnemann, Chem. Rev. 95 (1995) 69–96.
[42] A.-G. Rincon, C. Pulgarin, Appl. Catal. B: Environ. 51 (2004) 283–302.
[43] M. Abdullah, G.K.C. Low, R.W. Matthews, J. Phys. Chem. 94 (1990) 6820.

[44] P.-C. Maness, S. Smolinski, D.M. Blake, Z. Huang, E.J. Wolfrum, W.A. Jacoby, Appl. Environ. Microbiol. 65 (1999) 4094–4098.
[45] A.G. Rincon, C. Pulgarin, Appl. Catal. B: Environ. 44 (2003) 263–284.
[46] L. Zhang, J.C. Yu, H.Y. Yip, Q. Li, K.W. Kwong, A.-W. Xu, P.K. Wong, Langmuir 19 (2003) 10372–10380.
[47] M.M. Kondo, W.F. Jardim, Water Res. 25 (7) (1991) 823–827.
[48] W. Lee, H.-S. Shen, K. Dwight, A. Wold, J. Solid State Chem. 106 (1994) 288–294.
[49] L.-C. Chen, T.-C. Chou, Ind. Eng. Chem. Res. 33 (1994) 1436–1443.
[50] J.-M. Herrmann, H. Tahiri, Y. Ait-Ichou, G. Lassaletta, A.R. Conzalez-Elipe, A. Fernandez, Appl. Catal. B: Environ. 13 (1997) 219–228.
[51] M. Sokmen, D.W. Allen, F. Akkas, N. Kartal, F. Acar, Water Air Soil Pollut. 132 (2001) 153–163.
[52] A. Sclafani, M.N. Mozzanega, P. Pichat, J. Photochem. Photobiol. A: Chem. 59 (2) (1991) 181–189.
[53] E. Szabo-Bardos, H. Czili, A. Horvath, J. Photochem. Photobiol. A: Chem. 154 (2003) 195–201.
[54] H. Tsuji, H. Sugahara, Y. Gotoh, J. Ishikawa, Nucl. Instrum. Meth. Phys. Res. B 206 (2003) 249–253.
[55] H. Tsuji, T. Sagimori, K. Kurita, Y. Gotoh, J. Ishikawa, Surf. Coat. Technol. 158–159 (2002) 208–213.
[56] A. Dobosz, A. Sobczynski, Water Res. 37 (2003) 1489–1496.
[57] I.M. Arabatzis, T.S.M.C. Bernard, D. Labou, S.G. Neophytides, P. Falaras, Appl. Catal. B: Environ. 42 (2003) 187–201.
[58] H.M. Sung-Suh, J.R. Choi, H.J. Hah, S.M. Koo, Y.C. Bae, J. Photochem. Photobiol. A: Chem. 163 (2004) 37–44.
[59] D. Shchukin, E. Ustinovich, D. Sviridov, P. Pichat, Photochem. Photobiol. Sci. 3 (2004) 142–144.
[60] A. Ozkan, M.H. Ozkan, R. Gurkan, M. Akcay, M. Sokmen, J. Photochem. Photobiol. A: Chem. 163 (2004) 29–35.
[61] K.V.S. Rao, B. Lavedrine, P. Boule, J. Photochem. Photobiol. A: Chem. 154 (2003) 189–193.
[62] A.L. Semikina, V.P. Skulachev, FEBS Lett. 269 (1990) 69–72.
[63] J. Keleher, J. Bashant, N. Heldt, L. Johnson, Y. Li, World J. Microbiol. Biotechnol. 18 (2002) 133–139.